Low-energy tests of QED: Lamb shift

L&R, Physical Review 79.549 (1950)

FIG. 19. Cross section of apparatus. A. Tungsten oven of hydrogen dissociator. B. Shields. C. Anode of electron bombarder. D. Bombardment region. E. Accellerator grid of electron bombarder. F. Control grid. G. Cathode of electron bombarder. H. Heater for cathode. I. Slits. J. Wave guide. K. Quenching wires and transmission lines. L. Metastable detector target. M. Electron collector.

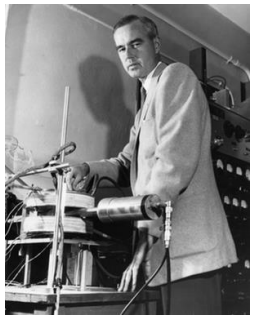

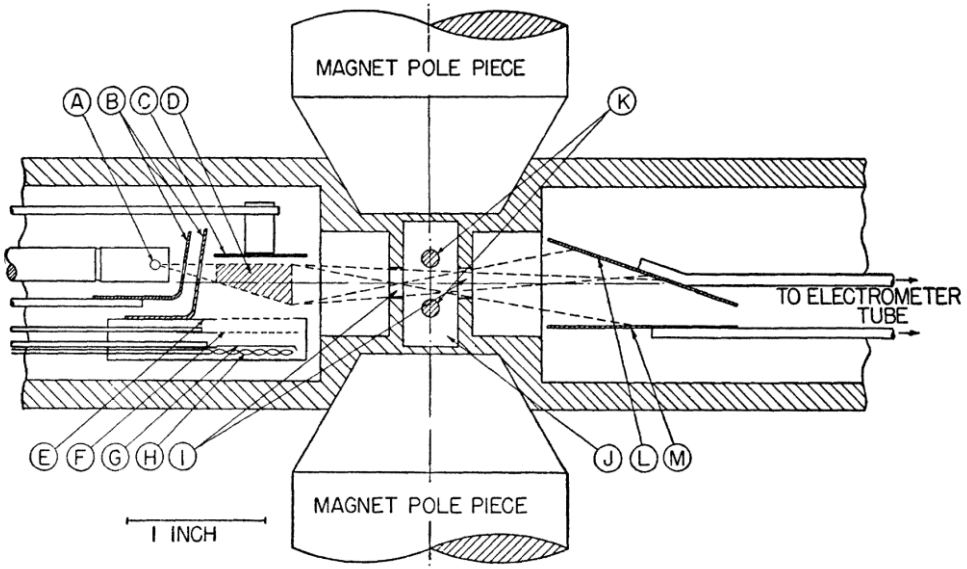

$$W_{ns}' = \frac{8}{3\pi}\left(\frac{e^2}{\hbar c}\right)^3 \mathrm{Ry}\frac{Z^4}{n^3}\ln\frac{K}{\langle E_n - E_m\rangle_{\mathrm{Av}}} = 1040 \text{ megacycles}$$

Bethe, Physical Review 72.339 (1947)

L&R, Physical Review 72.241 (1947)

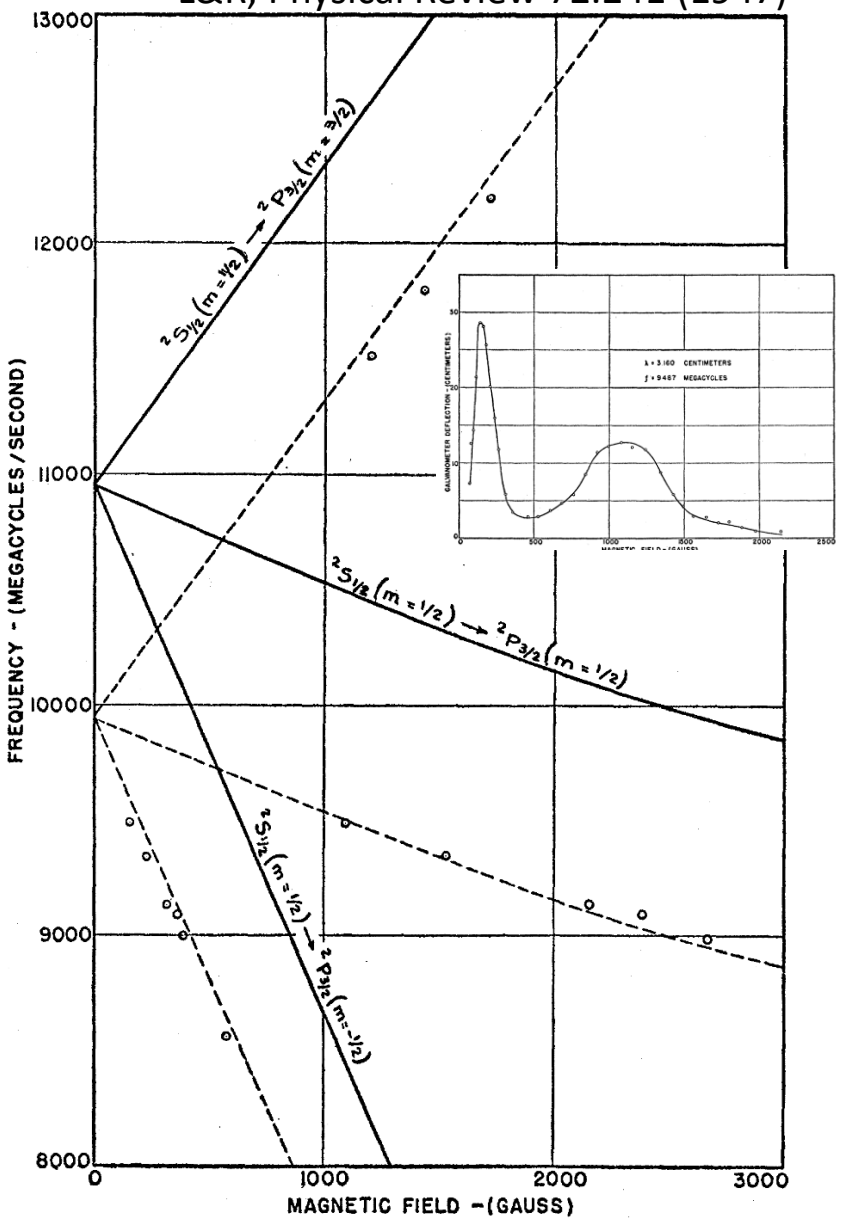

Low-energy tests of QED: Lamb shift

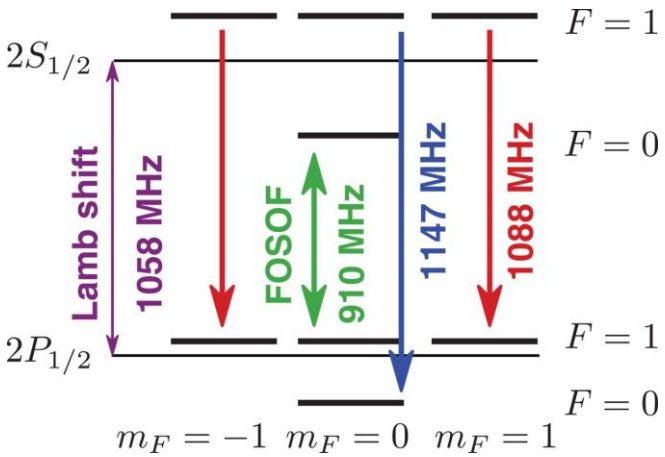

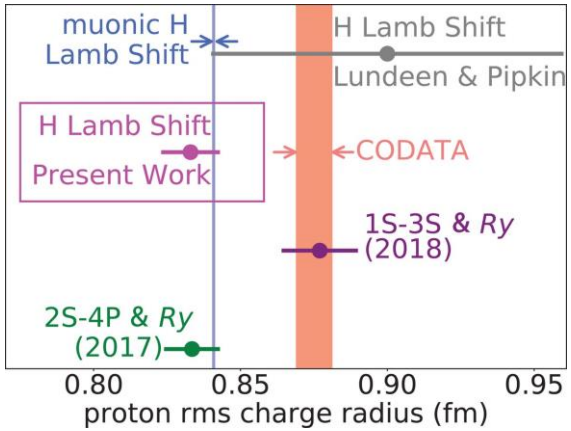

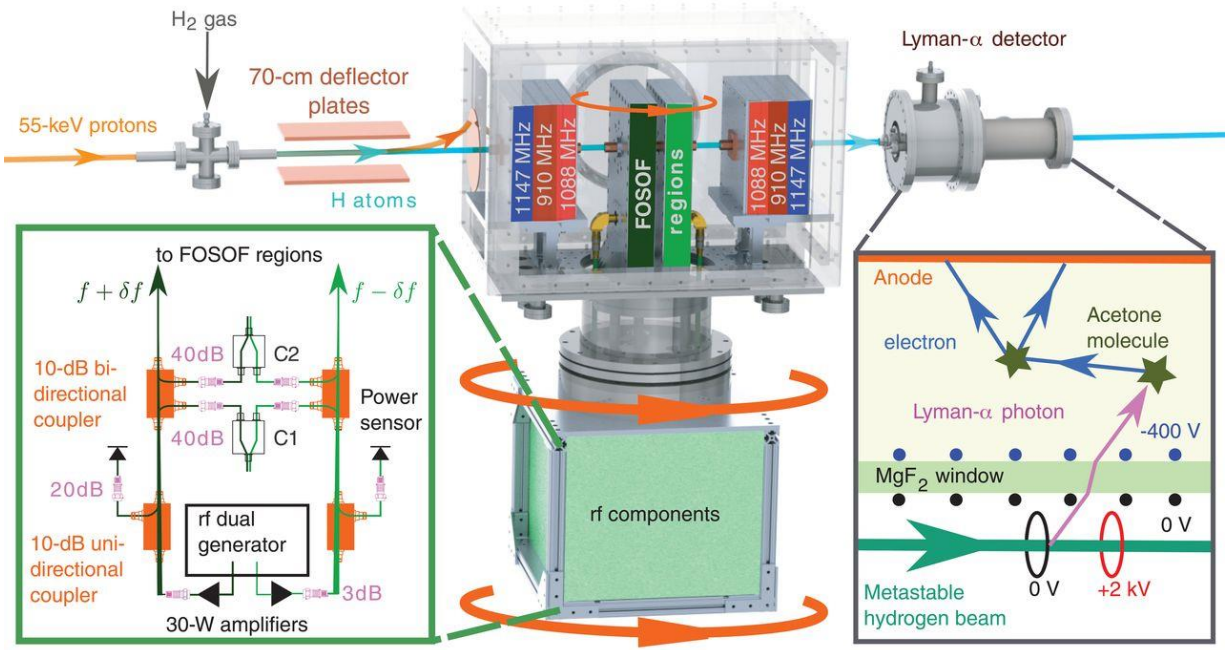

Science 365(6457), 1007-1012 (2019)

Low-energy tests of QED: Lamb shift

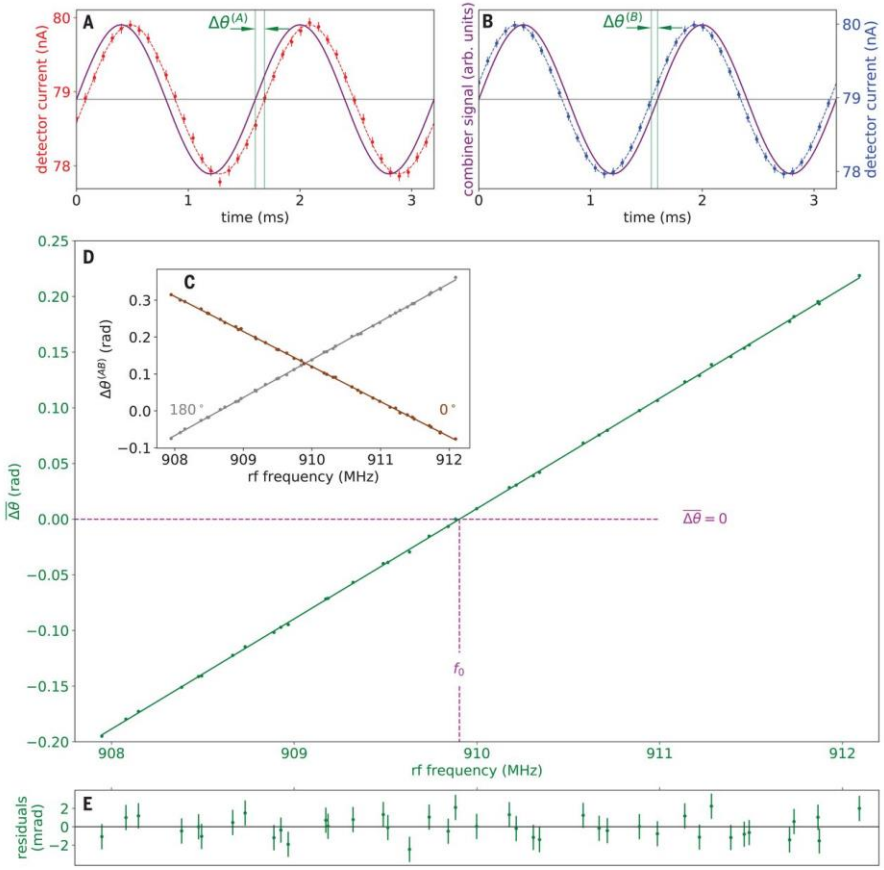

Fig. 3 The FOSOF signal.
(**A** and **B**) The FOSOF technique measures the phase difference Δθ between the atomic signal [red and blue in (A) and (B), respectively] and the reference signal (purple). The sign of Δθ depends on whether the atoms first encounter the $f + \delta f$ or $f - \delta f$ rf fields. In particular, in (A) the atoms first travel through the rf field region of frequency $f - \delta f$ and then through the field region of frequency $f + \delta f$. For the plot in (B), the order of the encountered frequencies is reversed. $|\Delta\theta^{(A)}|$ is larger than $|\Delta\theta^{(B)}|$ because of a phase offset caused by the limited bandwidth of the detection system. (**C**) The average of $\Delta\theta^{(A)}$ and $-\Delta\theta^{(B)}$ cancels this phase offset and is shown versus f for the two orientations of the FOSOF regions. (**D**) Average of Δθ(0°) (brown) and −Δθ(180°) (gray). The straight-line fit determines the f_0 at which Δθ = 0. (**E**) The residuals from the fit in (D) show that the data are fit well [$\chi^2(39) = 29.1$] by a simple straight line.

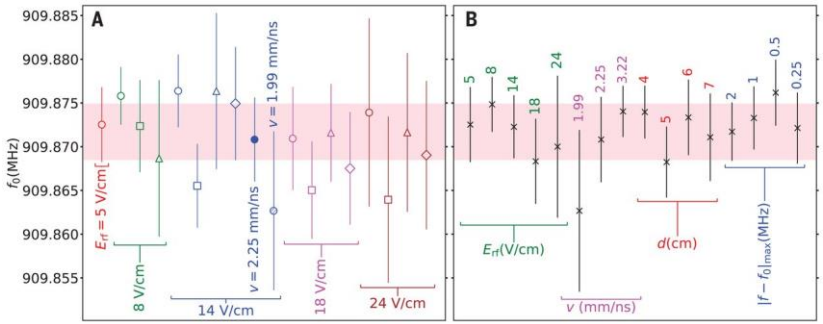

Fig. 4 Observed values for the atomic resonant frequency, f_0.
(**A**) Consistent centers are found for the 18 (v, d, E_{rf}) parameter sets used. Circles, squares, triangles, and diamonds represent d = 4, 5, 6, and 7 cm, respectively. (**B**) Averaged f_0 values for each v, d, and E_{rf} also agree, as do f_0 values obtained with the use of different frequency ranges. The pink band shows the 1σ uncertainty range for the current measurement. Numbers above the data points in (B) give the value of the parameters listed below the data points.

Science 365(6457), 1007-1012 (2019)

Low-energy tests of QED: Antihydrogen

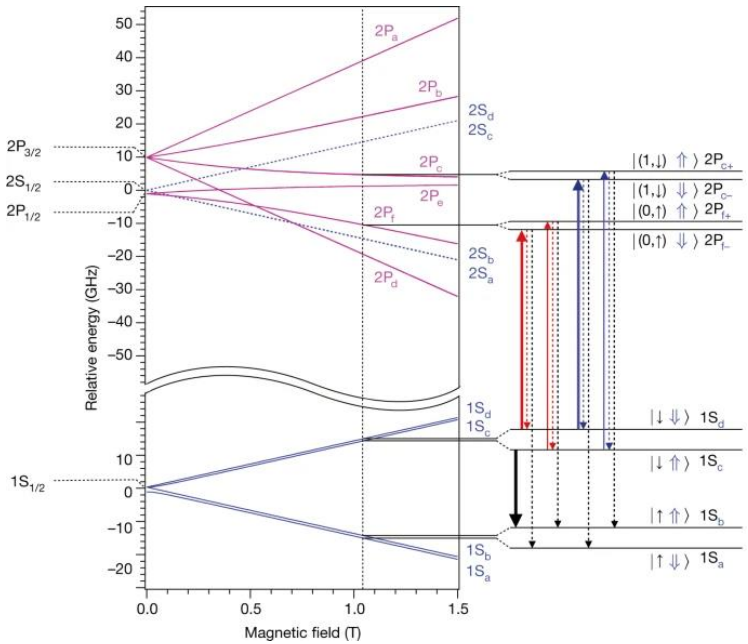

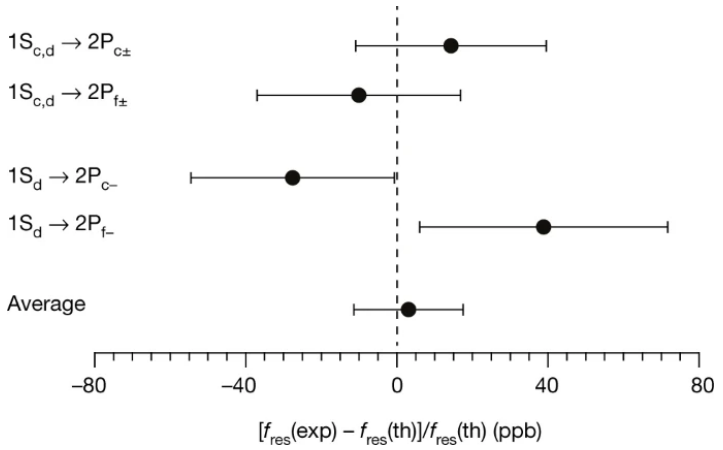

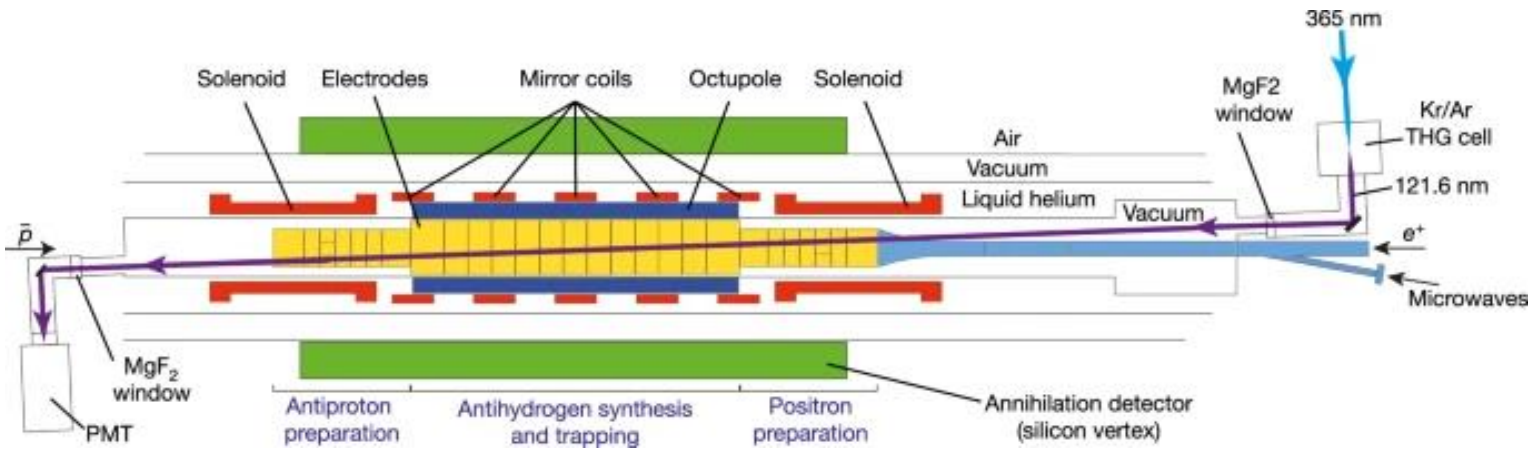

Nature 578, 375–380 (2020)

Low-energy tests of QED: Muonium

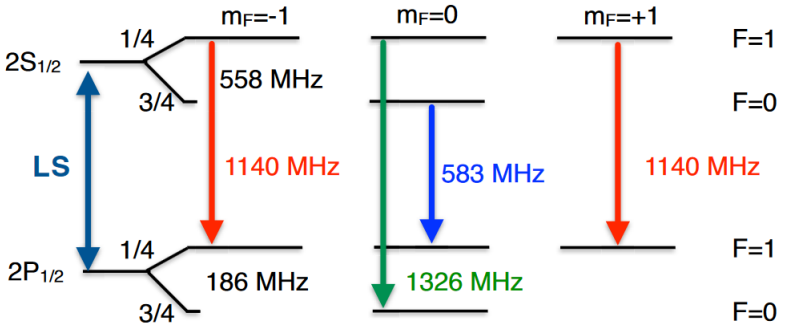

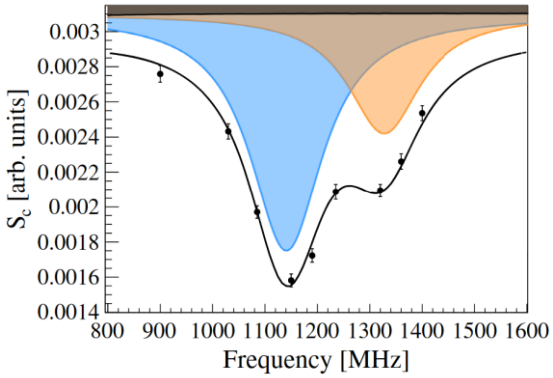

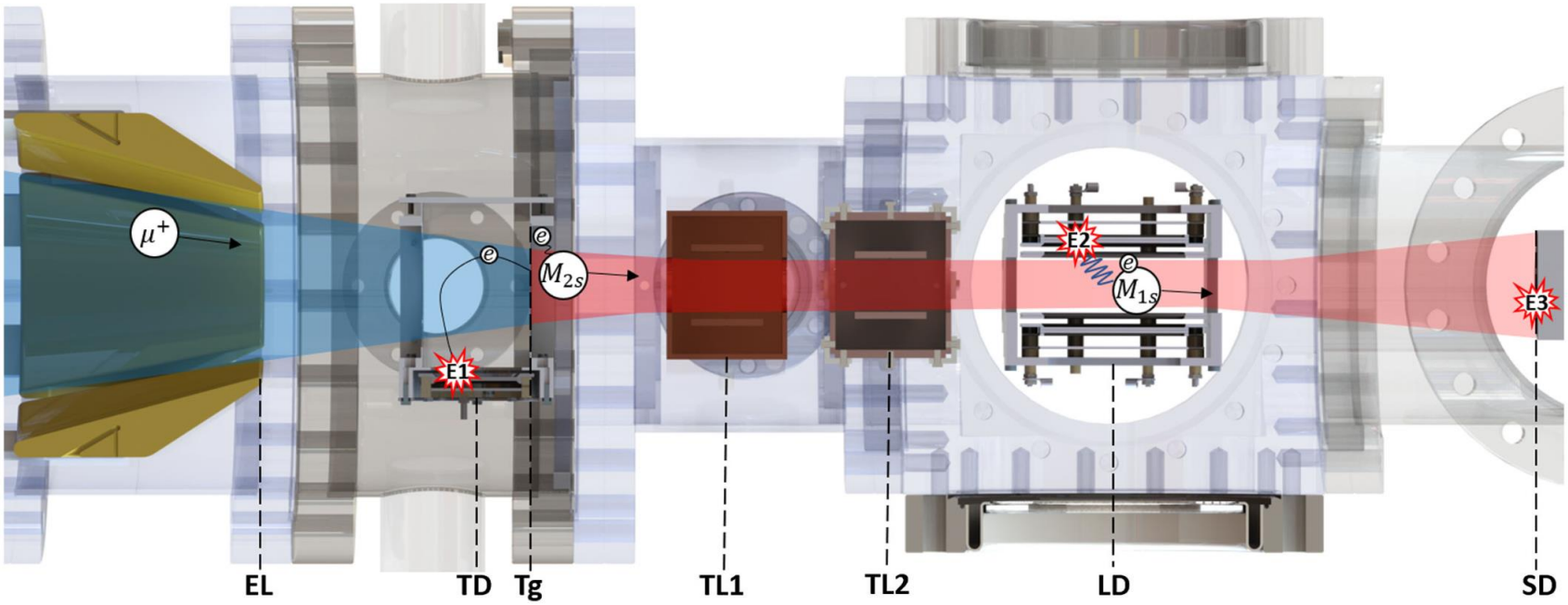

FIG. 1. Main elements of the experimental system. Conical electrostatic lens (EL), tagging detector (TD), carbon foil target (Tg), transmission line (TL), Lyman-alpha detector (LD), stop detector (SD). The normalization signal is given by the coincidence between an event in TD (E1) and SD (E3) within the expected time of flight, while a valid event includes also a reading in LD (E2).

PRL 128, 011802 (2022)

Low-energy tests of QED: Muonium

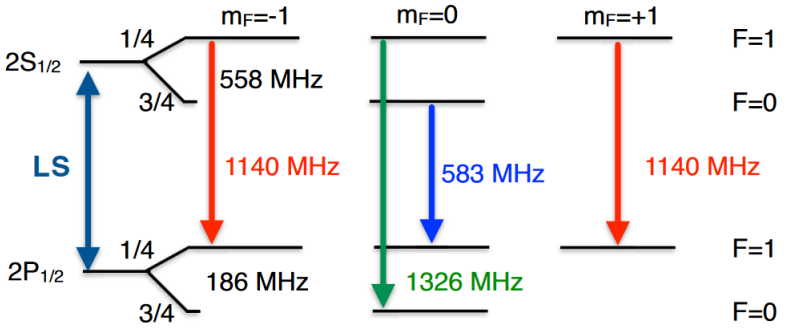

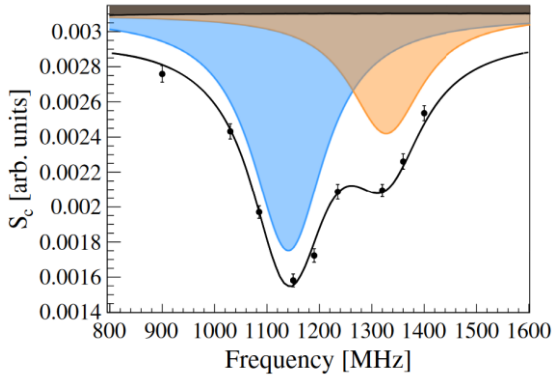

TABLE I. Central values and uncertainty contributions in MHz.

	Central value	Uncertainty
Fitting	1139.9	2.3
4S contribution		<1.0
MW-beam alignment		<0.32
MW field intensity		<0.04
M velocity distribution		<0.01
ac Stark $2P_{3/2}$	+0.26	<0.02
2nd-order Doppler	+0.06	<0.01
Earth's field		<0.05
Quantum interference		<0.04
$2S_{F=1} - 2P_{1/2,F=1}$	1140.2	2.5
Hyperfine	−93.0	0.0
Lamb shift	1047.2	2.5
Theoretical value [13]	1047.284	0.002

$$V_{ss}(\vec{r}) = -g_e^s g_\mu^s \frac{e^{-m_s r}}{4\pi r}$$

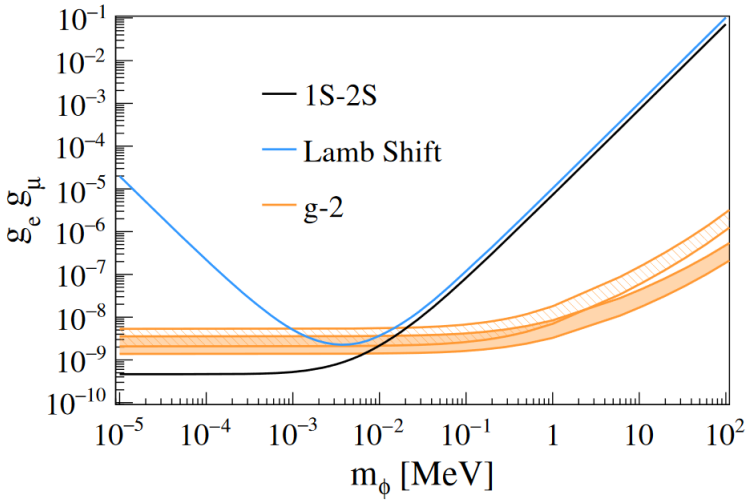

PRL 128, 011802 (2022)

Low-energy tests of QED: Heavy ions

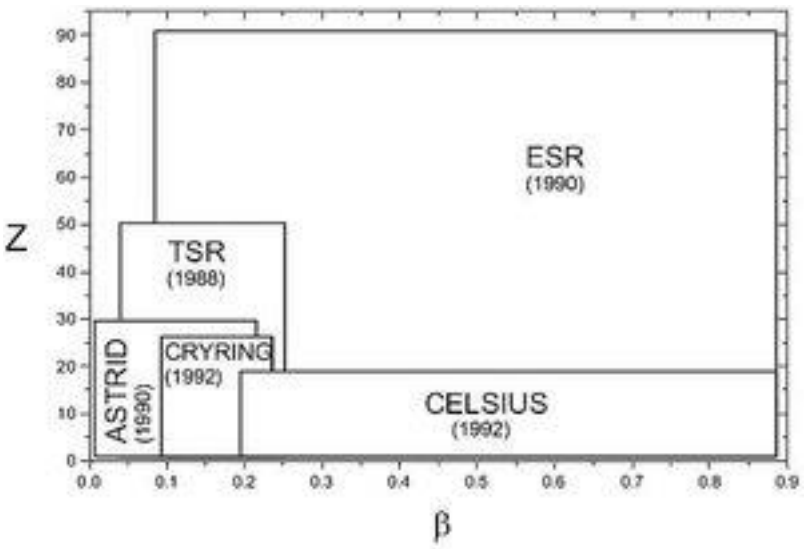

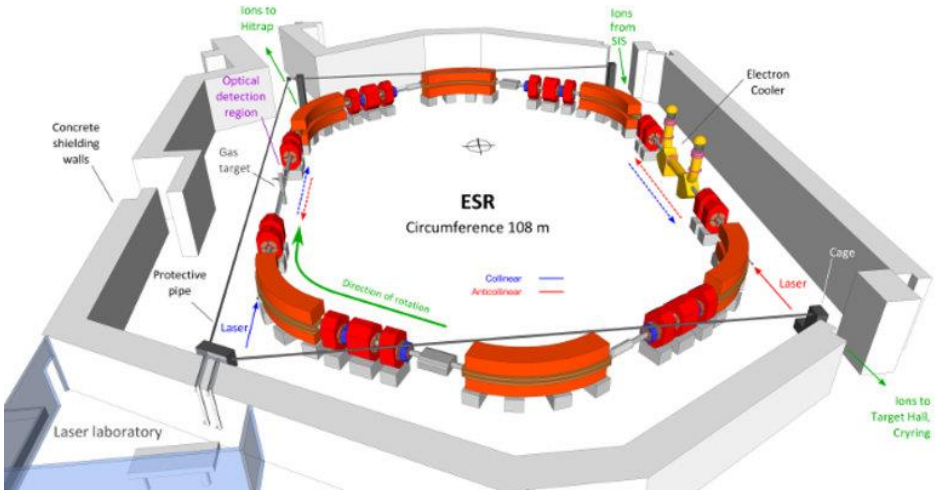

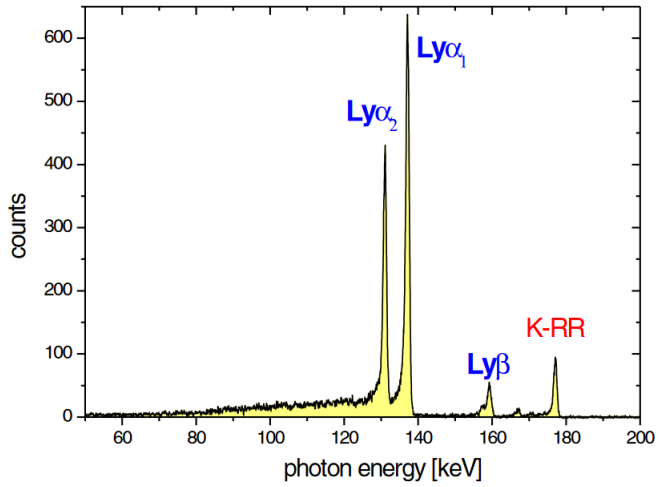

FIG. 1 (color online). X-ray spectrum (laboratory frame) following the radiative recombination of electrons with bare uranium ions.

PRL 94, 223001 (2005)

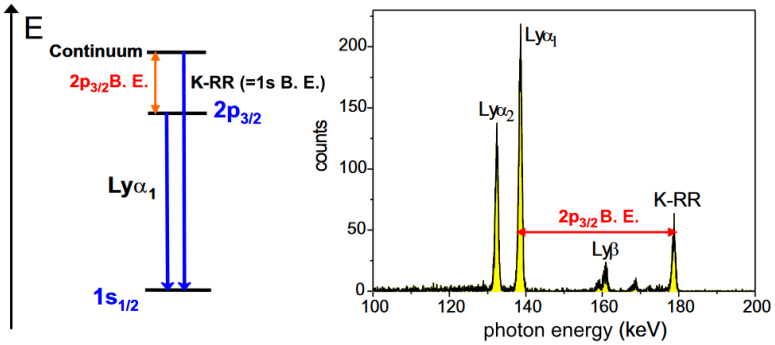

TABLE III. The ground-state Lamb shift in eV for H-like uranium.

Finite nuclear size	198.81
1st order QED	266.45
2nd order QED	−1.26(33)
Total theory [11,12]	464.26 ± 0.5
This work	460.2 ± 4.6

Low-energy tests of QED: muonic H

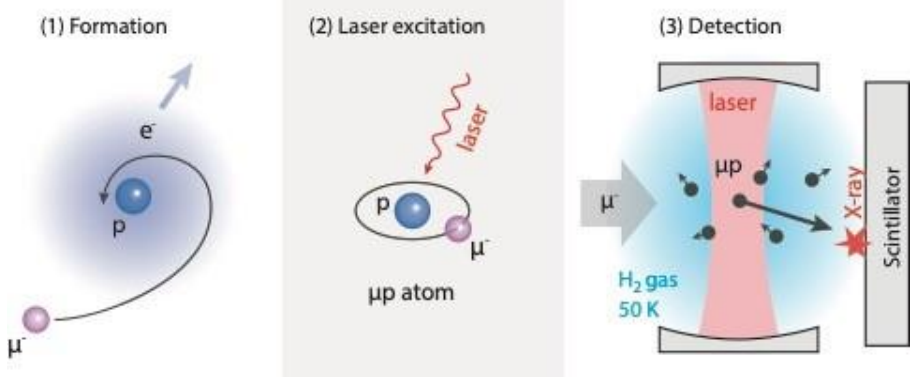

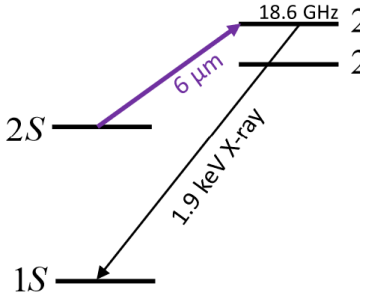

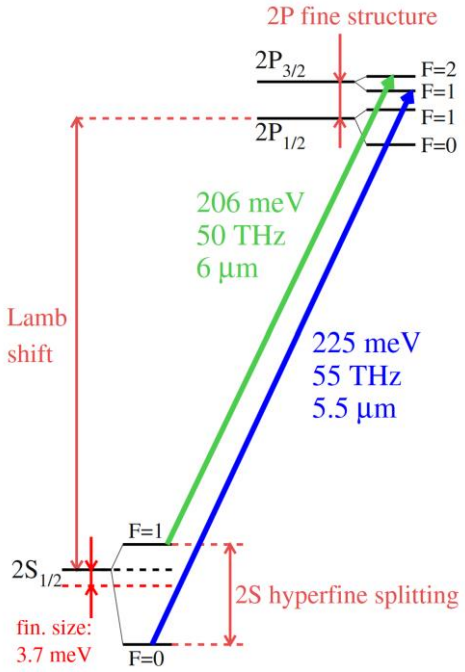

Protonic H:

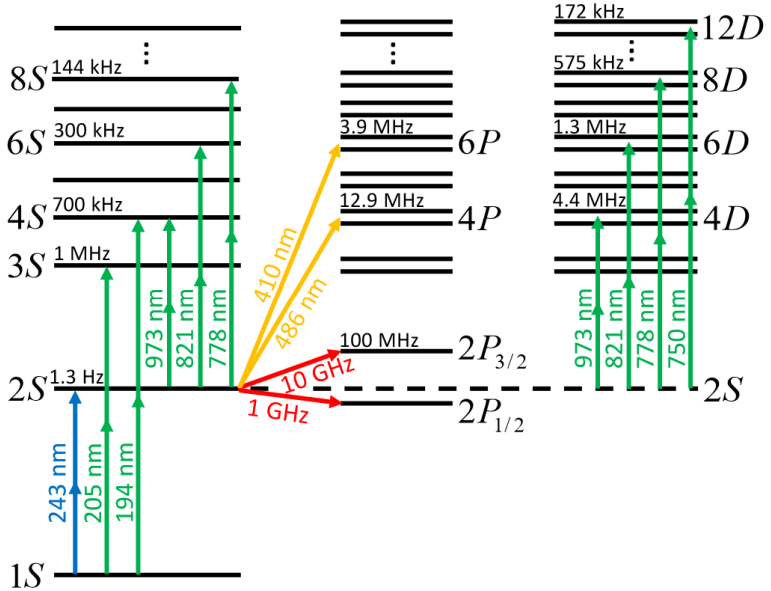

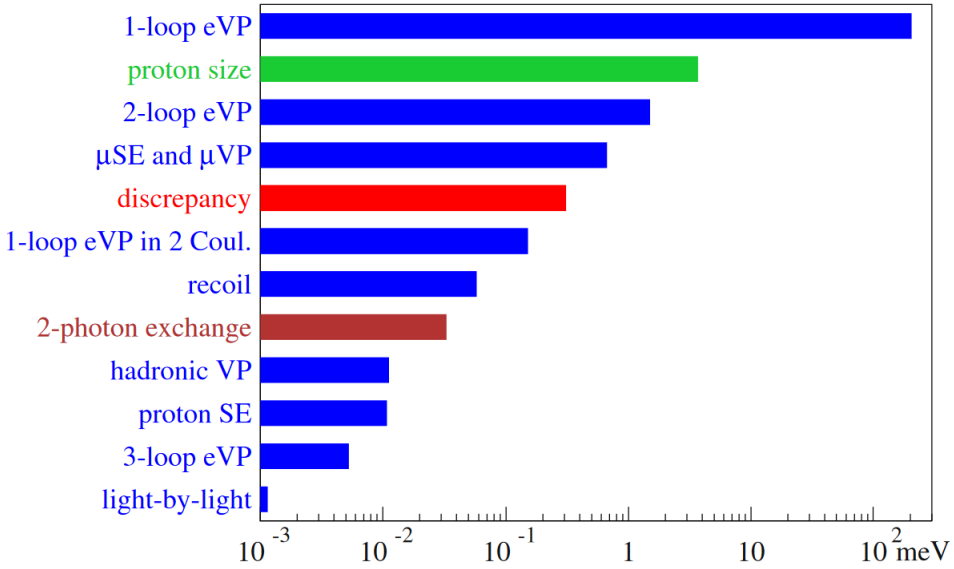

Low-energy tests of QED: muonic H

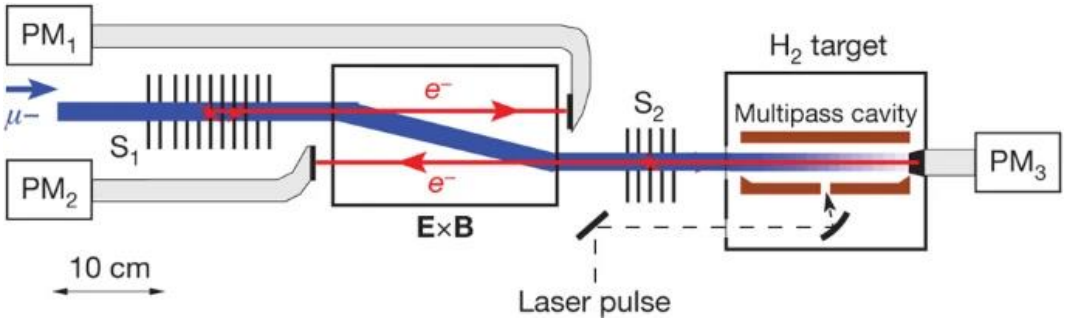

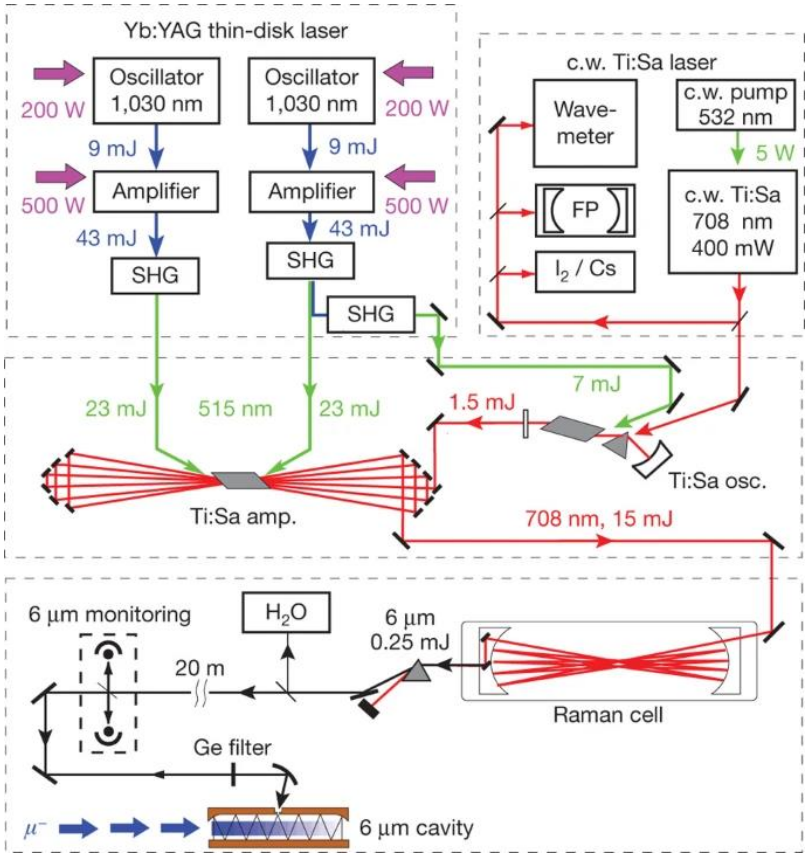

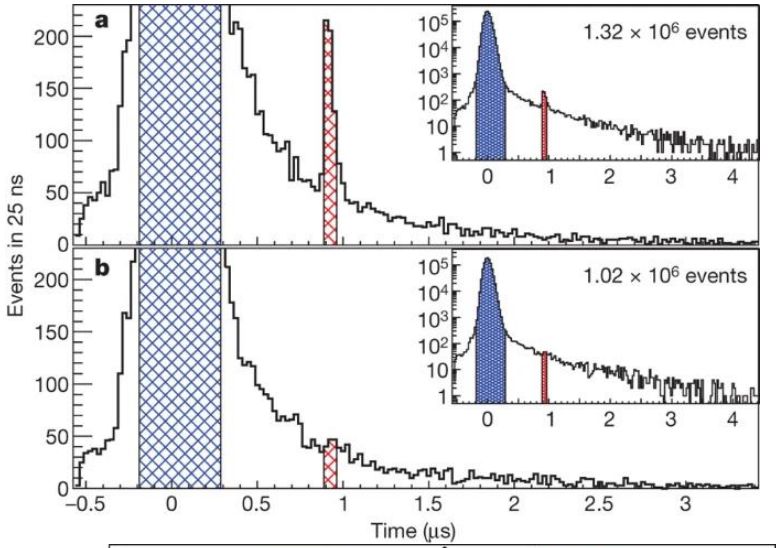

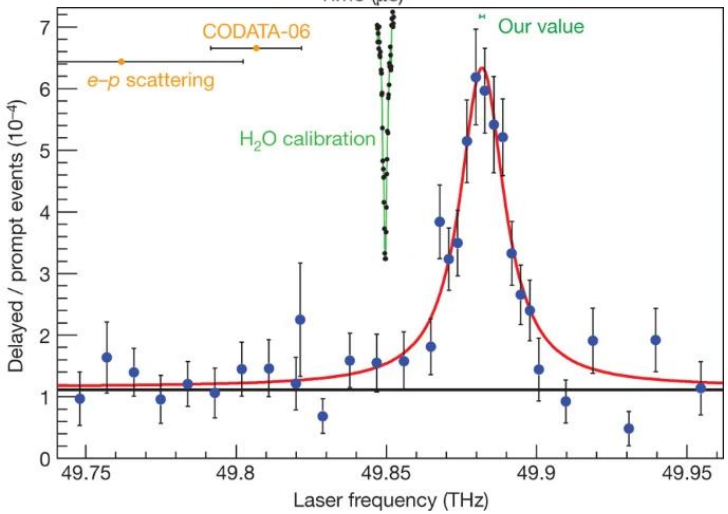

Nature 466, 213–216 (2010)

Low-energy tests of QED: Form factors

$$\mathscr{L}_{\text{fermion}} = -\frac{\mu}{2}\bar{\psi}\sigma^{\mu\nu}F_{\mu\nu}\psi - i\frac{d}{2}\bar{\psi}\sigma^{\mu\nu}\gamma^5 F_{\mu\nu}\psi$$

MDM **EDM**

$$\begin{aligned}\langle p_f|\, j^\mu \,|p_i\rangle = \bar{u}(p_f)\Big[&F_1(q^2)\gamma^\mu \\ &+ \frac{i\sigma^{\mu\nu}}{2m}q_\nu F_2(q^2) \\ &+ i\epsilon^{\mu\nu\rho\sigma}\sigma_{\rho\sigma}q_\nu F_3(q^2) \\ &+ \frac{1}{2m}\left(q^\mu - \frac{q^2}{2m}\gamma^\mu\right)\gamma_5 F_4(q^2)\Big]u(p_i)\end{aligned}$$

$$d = -\frac{F_3(0)}{2m} \qquad Q = F_1(0)$$

$$\mu = \frac{F_1(0)+F_2(0)}{2m} \qquad a = F_4(0)$$